Journal of *Marine Science and Engineering*

MDPI

Article

Chaotic Phase Modulation Direct-Sequence Spread Spectrum-Assisted Adaptive Serial Cancellation List Decoding Method for Underwater Acoustic Communication

Yuan Sun [1], Danyang Hong [2,3,*], Dong Liu [1,4] and Jinyu Lei [5,*]

1 College of Physics and Electronic Information Engineering, Minjiang University, Fuzhou 350108, China
2 Institute of Acoustics, Chinese Academy of Sciences, Beijing 100190, China
3 Key Laboratory of Science and Technology on Advanced Underwater Acoustic Signal Processing, Chinese Academy of Sciences, Beijing 100190, China
4 Department of Mechanical Engineering, Tsinghua University, Beijing 100084, China
5 College of Computer and Data Science, Minjiang University, Fuzhou 350108, China
* Correspondence: hongdanyang17@mails.ucas.ac.cn (D.H.); j.lei@mju.edu.cn (J.L.)

Abstract: Addressing the challenges of high decoding latency, reduced spectral efficiency, and substantial storage requirements in a Cyclic Redundancy Check (CRC)Aided Successive Cancellation List (CA-SCL) polar decoder, this paper proposes a chaotic phase modulation direct-sequence spread spectrum (CPMDSSS)-assisted adaptive serial cancellation list decoding method for underwater acoustic communication. The method involves segmenting the information bits to be transmitted, computing CRC for each segment, and mapping all CRCs to a CPMDSSS, which is then modulated onto the pilot subcarriers of underwater acoustic orthogonal frequency-division multiplexing (OFDM) to increase spectral efficiency. At the receiving end, CRCs are obtained by demodulating the CPMDSSS to verify the segmented information and adaptively select the number of decoding paths. The theoretical analysis and simulation results demonstrate that compared to CA-SCL, the proposed method effectively reduces the required storage units and improves spectral efficiency, with an average reduction of approximately 80% in the decoding paths. Sea trials further indicate that the proposed method reduces the average decoding paths by approximately 71% and decreases the average decoding delay by approximately 64% compared to CA-SCL.

Keywords: polar codes; chaotic phase modulation direct-sequence spread spectrum; adaptive decoding; SCL decoder; underwater acoustic communications

check for updates

Citation: Sun, Y.; Hong, D.; Liu, D.; Lei, J. Chaotic Phase Modulation Direct-Sequence Spread Spectrum-Assisted Adaptive Serial Cancellation List Decoding Method for Underwater Acoustic Communication. *J. Mar. Sci. Eng.* **2024**, *12*, 948. https://doi.org/10.3390/jmse12060948

Academic Editor: Sergei Chernyi

Received: 5 May 2024
Revised: 31 May 2024
Accepted: 3 June 2024
Published: 5 June 2024

Copyright: © 2024 by the authors. Licensee MDPI, Basel, Switzerland. This article is an open access article distributed under the terms and conditions of the Creative Commons Attribution (CC BY) license (https://creativecommons.org/licenses/by/4.0/).

1. Introduction

The complex characteristics of underwater acoustic channels require the implementation of effective channel coding techniques to significantly improve system performance and ensure reliable communication. The prevalent coding schemes for underwater acoustic channels include Turbo codes, Low Density Parity Check Codes (LDPC), convolutional codes, and RS codes. Notably, LDPC codes demonstrate commendable performance, especially when used with long codewords and soft-decision decoding techniques. However, LDPC codes still exhibit a slight deviation of approximately 0.0045 dB from the Shannon theoretical limit. The concept of channel polarization led to the development of polar codes by Arıkan in 2009 [1]. As a type of linear block codes, polar codes offer the advantage of reduced encoding and decoding complexity. When applied to Binary Discrete Memoryless Channels (BDMC), polar codes can achieve the Shannon limit, attracting significant scholarly attention [2–5].

Polar decoders play a crucial role in the performance of communication systems, garnering continuous attention from scholars [6–13]. Arıkan proposed the Successive Cancellation (SC) decoding method, widely adopted due to its lower decoding complexity

($O(N \log N)$) [6]. However, SC decoders exhibit serious error propagation issues, leading to decreased decoding performance, especially with shorter code lengths. To address this issue, Tal et al. proposed the Successive Cancellation List (SCL) decoder, where up to L decoding paths are concurrently considered at each decoding stage, and then a single codeword is selected from the list as the output [7]. Building upon SCL, Kai et al. introduced the Cyclic Redundancy Check Aided Successive Cancellation List (CA-SCL), which cascades CRC with polar codes, further reducing the bit error rate [8]. However, the complexity of CA-SCL increased to $O(LN \log N)$, and the additional CRC, sacrifices the spectral efficiency. In order to reduce the decoding complexity of CA-SCL, segmented CRC was employed. Nevertheless, the decoding path for each information segment remained at L, resulting in insignificant complexity reduction [9]. In hardware implementation, compared to CA-SCL, the Partitioned SCL (PSCL) decoder reduced power consumption and storage unit utilization but sacrificed error correction performance [10]. The Simplified SCL (SSCL) decoder [11] and the Fast Simplified SCL (Fast-SSCL) decoder [12] aimed to reduce decoding latency, relying on bit pattern recognition to prune the SC decoding tree and reduce the required number of estimated bits. However, both suffered from decreased error correction performance. Traditional CA-SCL and its derivative methods often choose to retain more paths for better error correction performance, leading to higher computational complexity and latency. The Adaptive SCL (AD-SCL) decoder, based on CA-SCL, adapts the number of retained paths for re-decoding based on the CRC check results of the decoding sequence, reducing the overall decoding complexity while achieving good decoding performance [13]. This represents a promising decoding approach.

To address the challenges mentioned in the above, including high decoding latency, reduced spectrum efficiency, and substantial storage requirements in polar decoder, this paper introduces a novel chaotic phase modulation direct-sequence spread spectrum (CPMDSSS)-assisted adaptive SCL decoding method for underwater acoustic communication. The main contributions of this research can be summarized as follows:

1. Proposal of a novel decoding method integrating CPMDSSS with an SCL decoder for underwater acoustic OFDM communication. The method involves segmenting the information bits to be transmitted, computing CRC for each segment, and mapping all CRCs to a CPMDSSS, which is then modulated onto the pilot subcarriers of underwater acoustic orthogonal frequency-division multiplexing (OFDM) to increase spectrum efficiency.
2. The proposed method checks CRCs and adaptively selects the number of decoding paths for each information segment. Compared to traditional CA-SCL decoders, the proposed method reduces the decoding latency and storage requirements.

The remainder of this article is organized as follows: Section 2 provides a brief overview of polar encoders and decoders. Section 3 introduces the proposed polar decoder for underwater acoustic OFDM communication and provides the performance analysis. Section 4 presents the simulation and sea trial results and provides an analysis of these finding. Finally, Section 5 concludes the entire paper.

2. Polar Coder and Decoder

2.1. Construction of Polar Code

The construction of polar codes can be divided into three steps: (1) determining polarized channels; (2) generating the generator matrix; (3) executing the polar codes' encoding [6,14,15]. The selection of polarizing subchannels based on Gaussian Approximation (GA) is the commonly used method for subchannel selection [15]. Under the premise of Gaussian channels, GA allocates K information bits u_A to the most reliable bit channels following a channel reliability assessment, and sets the (N-K) frozen bits u_{AC} to the unreliable channels. Then, the source binary vector can be denoted as $u_1^N = (u_A, u_{AC}) = \{u_1, u_i, \ldots, u_N\}$. In subsequent discussions, the notation A_i^j is used to denote the vector $\{a_i, a_{i+1}, \ldots, a_j\}$.

Perform linear encoding on the source vector u_1^N, thereby obtaining the codeword vector x_1^N:

$$x_1^N = u_1^N G_N, \tag{1}$$

where the generator matrix is $G_N = B_N F^{\otimes \log_2 N}$ of codeword length N, and $\otimes$ represents the Kronecker product; B_N is the bit-reversal permutation vector; and the kernel matrix is F:

$$F = \begin{pmatrix} 1 & 0 \\ 1 & 1 \end{pmatrix}. \tag{2}$$

Then, the codeword x_1^N is modulated by OFDM and is transmitted through the underwater acoustic channel. The receiving end receives the codeword y_1^N after demodulating OFDM.

2.2. SC Decoder

As a classic decoding method for polar codes [6], the SC decoder involves iteratively decoding the polar codes of length N as its core principle. It utilizes the received codeword y_1^N and the previously decoded information bits u_1^{i-1} to jointly decode u_i until decoding reaches u_N. The decoding process for u_i is expressed as follows:

First, compute the log likelihood ratio (LLR) of the received signal, and then decode u_i based on $LLR_N^{(i)}$, where $LLR_N^{(i)}$ denotes the LLR of the i-th polarized channel in the N polarized channel.

$$u_i = \begin{cases} 0, \ LLR_N^{(i)} > 0 \\ 1, \ LLR_N^{(i)} < 0 \end{cases}. \tag{3}$$

Under the BDMC channel W, after the polarization of the channel, the channel $W_N(y \mid x)$ is obtained through channel combining. By splitting $W_N(y \mid x)$, the polarized channels $W_N^{(i)}$ $\{1 \le i \le N\}$ are obtained. Then, the $LLR_N^{(i)}$ can be expressed as follows:

$$LLR_N^{(i)} = \ln\left(\frac{W_N^{(i)}(y_1^N, u_1^{i-1} | u_i = 0)}{W_N^{(i)}(y_1^N, u_1^{i-1} | u_i = 1)}\right). \tag{4}$$

Equation (5) provides the recursive relationship for the polarized channel $W_N^{(i)}$:

$$\begin{aligned} W_N^{(2i-1)}(y_1^N, u_1^{2i-2} | u_{2i-1}) &= \frac{1}{2}\sum_{u_{2i}} W_{N/2}^{(i)}(y_1^{N/2}, u_{1,o}^{2i-2} \oplus u_{1,e}^{2i-2} | u_{2i-1} \oplus u_{2i}) W_{N/2}^{(i)}(y_{N/2+1}^N, u_{1,e}^{2i-2} | u_{2i}), \\ W_N^{(2i)}(y_1^N, u_1^{2i-1} | u_{2i}) &= \frac{1}{2} W_{N/2}^{(i)}(y_1^{N/2}, u_{1,o}^{2i-2} \oplus u_{1,e}^{2i-2} | u_{2i-1} \oplus u_{2i}) W_{N/2}^{(i)}(y_{N/2+1}^N, u_{1,e}^{2i-2} | u_{2i}), \end{aligned} \tag{5}$$

where $u_{1,o}^{2i-2}$ represents the elements with an odd index in u_1^{2i-2}; $u_{1,e}^{2i-2}$ represents the elements with an even index in u_1^{2i-2}; $\oplus$ represents modulo 2 operation.

By utilizing Equations (3)–(5), SC decoding can be performed recursively. Through the decoding process described above, it can be seen that the SC decoder employs recursive decoding, which introduces the drawback of error propagation. This means that the impact of a decoding error in the previous step will propagate to the subsequent source decoding, resulting in an increased bit error rate.

2.3. CA-SCL Decoder

To mitigate the error propagation issue inherent in SC decoding, the CA-SCL decoder employs L SC decoders concurrently during the decoding process. It maintains the L most probable source estimation sequences based on the posterior probabilities obtained from decoding. Subsequently, the decoder selects the source sequence with the highest posterior probability and passes the CRC, thereby determining it as the final decoded sequence.

Assuming $P(u_1^i | y_1^N)$ represents the posterior probability of the i-th decoding result, and defining $-\ln(P(u_1^i | y_1^N))$ as the Path Metric (PM), the theorem in the literature [16] establishes the following:

$$PM = -\ln\left(P\left(u_1^i|y_1^N\right)\right) = \sum_{k=1}^{i} \ln\left(1 + e^{-(1-2u_k)LLR_N^{(k)}}\right). \quad (6)$$

Equation (6) shows that the PM can be represented by $LLR_N^{(1)}$, $LLR_N^{(2)}$, ..., $LLR_N^{(i)}$. This equation highlights the importance of maximizing the posterior probability $P\left(u_1^i|y_1^N\right)$ for achieving correct decoding results.

Figure 1 depicts the decoding process of CA-SCL. Frozen bits are set to 0 directly, and the PM is calculated accordingly. For information bits, both $u_i = 0$ and $u_i = 1$ outcomes are retained, and their respective PMs are also computed. As decoding proceeds, candidate decoding paths are generated. If the number of paths exceeds the limit L of the SC decoder, the L most reliable paths based on their PM values are selected as survivor paths. These L survivor paths are then involved in the subsequent decoding process, while the excess paths are discarded. Finally, the decoder selects the source sequence with the highest posterior probability and passes the CRC, thereby determining it as the final decoded sequence.

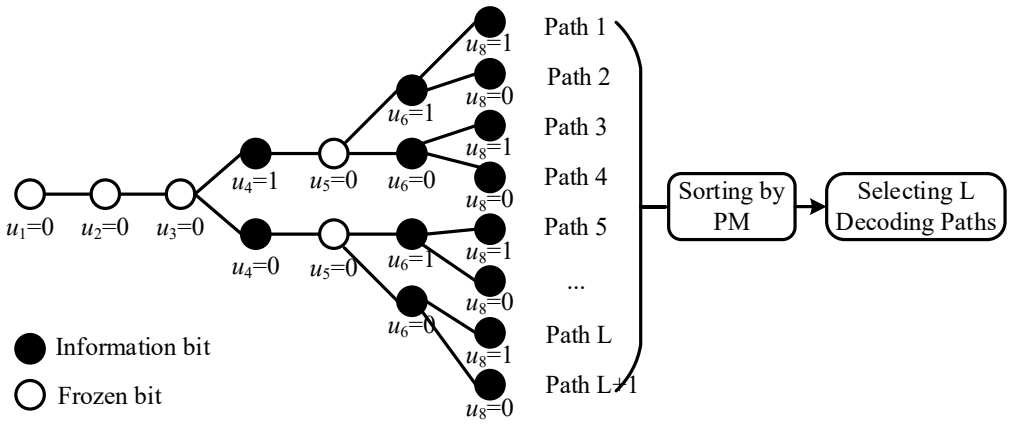

Figure 1. Schematic diagram of the SCL decoding process.

Upon analysis, it is clear that the CA-SCL decoder requires a significant number of storage units, and the fixed decoding path L leads to decreased decoding efficiency and longer decoding latency. Furthermore, adding extra CRC to the source vector u_1^N reduces the effective information bits, resulting in lower spectral efficiency.

3. The Proposal Method

The proposed method comprises three primary components: (1) the generation of chaotic phase modulation direct-sequence spread spectrum (CPMDSSS), (2) the encoding of polar codes, and (3) the decoding of polar codes. CPMDSSSs are employed as OFDM pilots, which are initially introduced in this section. Subsequently, the paper introduces the encoding and decoding processes.

3.1. Chaotic Phase Modulation Direct-Sequence Spread Spectrum

Traditional pseudo-random sequences, such as m-sequences [17] and Gold sequences [18], have a limited number of codebooks, making it difficult to cover all possible CRCs. However, by employing chaotic phase modulation direct-sequence spread spectrum, there is no limitation on the number of codebooks. Utilizing different initial values, a large number of chaotic spreading sequences with strong self-correlation can be generated [19]. Modulating the chaos phase onto the carrier phase can overcome the problem of periodicity and binary values caused by conventional PN sequences [20].

Utilizing the Quadratic Mapping Equation [21], the generation process of chaotic direct-sequence spread spectrum in this paper is outlined as follows:

$$g(m+1) = P - Qg^2(m), m = 0, 1, \ldots, J-1, \quad (7)$$

where P and Q are the parameters for generating chaotic spreading sequences and $g(m)$ represents the value of the direct-sequence spread spectrum. When $3/4 < PQ < 2$, then $g(m) \in (-2/Q, 2/Q)$. In this paper, the values of P and Q are set to $1/4$ and 4, respectively.

By utilizing the chaotic initial value $g(0)$ and Equation (7), a chaotic direct-sequence spread spectrum of length J, denoted as $\boldsymbol{g}^J = (g(0), g(1), g(2), \ldots, g(J-1))$, can be generated. Selecting K different $g(0)$ enables the generation of mutually orthogonal chaotic spreading sequences, denoted as:

$$\boldsymbol{g}_1^J, \boldsymbol{g}_2^J, \ldots, \boldsymbol{g}_K^J. \tag{8}$$

The generated sequences are then remapped onto the carrier phase, thereby generating CPMDSSS:

$$\boldsymbol{p}^J = \exp\left(j2\pi \boldsymbol{g}^J\right). \tag{9}$$

3.2. The Encoder of the Proposed Method

Figure 2 depicts the encoding process of the proposed method, which can be divided into the following steps:

Step 1: Divide the K information bits into M segments, defined as $\{l_1, \ldots, l_i, \ldots, l_M\}$. The larger the value of M, the better the performance obtained, but this also leads to a corresponding increase in the complexity of CRC and CPM demodulation. In practical experience, the value of M is usually less than 8.

Step 2: Generate corresponding binary $\mathrm{CRC}_{(i)}$ for each segment $\{l_1, \ldots, l_i, \ldots, l_M\}$, concatenate all binary CRC to obtain $\mathrm{CRC}_{total} = \{\mathrm{CRC}_{(1)} \ldots \mathrm{CRC}_{(i)} \ldots \mathrm{CRC}_{(M)},\}$, convert CRC_{total} into a signed binary number CRC^*_{total}, and obtain $g(0) = CRC^*_{total}/(2 \times CRC^*_{\max})$, where $CRC^*_{\max}$ is the maximum value within the range of CRC^*_{total}.

Step 3: Based on Formula (9), generate a CPMDSSS $\boldsymbol{p}^J$ corresponding to the $g(0)$ obtained in Step 2.

Step 4: Employ the Gaussian construction method [15] to establish reliable and unreliable bit channels, combine (N-K) frozen and K information bits, and generate a source vector of length N.

Step 5: Place the CPMDSSS $\boldsymbol{p}^J$ on the OFDM pilot positions. Additionally, the codewords are mapped to data subcarriers of OFDM. Then, the proposed method performs OFDM modulation, and ultimately generates the signal to be transmitted.

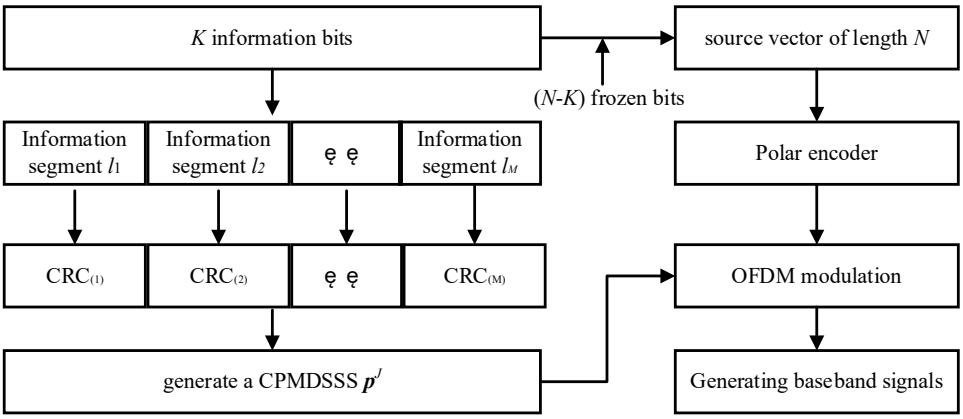

Figure 2. The encoding process of the proposed method.

3.3. The Decoder of the Proposed Method

Figure 3 depicts the decoding process of the proposed method, which can be divided into the following steps:

Step 1: To reduce the effects of the underwater acoustic multipath channel during the demodulation of CPMDSSS, the proposed method initially acquires an estimation of the underwater acoustic channel using LFM added to the transmitted signal. Then, it applies preliminary equalization [22,23] to the received OFDM signals, and extracts the received CPMDSSS based on the positions of OFDM pilots.

Step 2: Calculate the correlation between the local generated CPMDSSSs and the received CPMDSSS. Select the local CPMDSSS sequence with the highest correlation as the demodulated result to obtain $g(0)$. Using the inverse mapping described in Step 2 of Section 3.2, we can then obtain the CRCs corresponding to each information segment.

Step 3: Define n as the iteration index of decoding path $L'_{n.}$ Set the decoding path to L'_0 =1. Employ the SC decoder to decode the received codeword. If the l_i information segment passes the $CRC_{(i)}$, then the decoding of l_i is considered successful. If it fails the $CRC_{(i)}$, expand the decoding path to $L'_n = 2L'_{n-1}$ ($L'_n \leq L$) and execute Step 4 to re-decode the information bit l_i.

Step 4: During the decoding process, if the decoding path $L'_n \leq L$ and a decoded result passing the $CRC_{(i)}$ exists, then the decoding of l_i is considered successful. Otherwise, set $L'_n = 2L'_{n-1}$ ($L'_n \leq L$). Repeat Step 4, decoding until a decoded result passing the $CRC_{(i)}$ is obtained. If $L'_n > L$ during the decoding process, declare decoding failure.

Step 5: After successfully decoding the information segments $\{l_1, \ldots, l_i\}$, send them to the SC decoder in Step 3 to decode the l_{i+1} information segment. Repeat Steps 3 to 5 until decoding fails or all information segments have been successfully decoded.

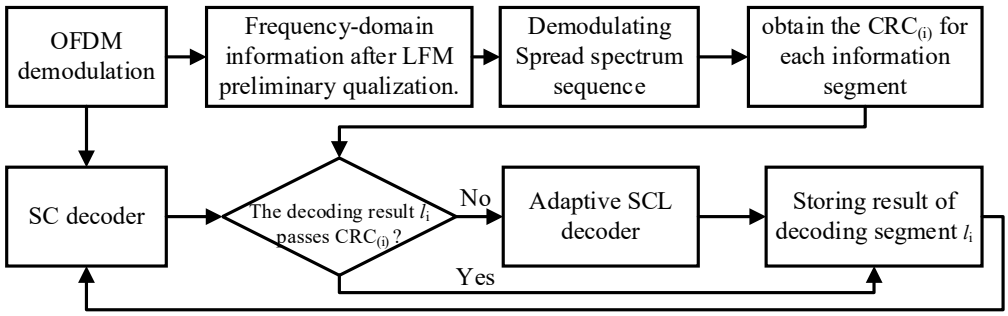

Figure 3. The decoding process of the proposed method.

3.4. Performance Analysis

3.4.1. Storage Space Requirements Analysis

In the traditional CA-SCL decoder, CRC can only be performed after decoding all K information bits, which prevents the early elimination of redundant decoding paths. Consequently, with L decoding paths, $K \times L$ information bits must be stored, denoted as $R_{CA-SCL} = K \times L$.

In the optimal decoding scenario described in this paper, where the first decoding path for each information segment successfully passes CRC, it requires storing K information bits. The necessary required storage units can be donated as $(R_{proposed})_{best} = K$.

In the worst case scenario, where each information segment requires L decoding paths to pass CRC, the L decoding paths need to store $(K/M) \times L$ information bits. Furthermore, approximately K storage units are needed to retain the decoded messages. Then, the necessary storage units can be donated as $(R_{proposed})_{worst} = (K/M) \times L + K$. The required storage units ratio between the proposed decoder and the CA-SCL decoder can be expressed as R_{mem}:

$$R_{mem} = \frac{R_{proposed}}{R_{CA-SCL}}, \ (R_{mem})_{optimal} = \frac{1}{L}, \ (R_{mem})_{worst} = \frac{1}{M} + \frac{1}{L}. \tag{10}$$

3.4.2. Decoding Complexity and Latency Analysis

Given the codeword of length N and the number of decoding paths L in the CA-SCL decoder, the computational complexity is $O(LN \log N)$. For simplifying the latency model, we assume that the decoding delay scales linearly with the decoding complexity. Therefore, the decoding latency of CA-SCL is expressed as:

$$T_{CA-SCL} = c \times L \times N \log N, \tag{11}$$

where c is the scaling factor.

Compared to the CA-SCL, the proposed decoder immediately outputs the sequence of an information segment l_i upon completing its decoding. Therefore, the average decoding delay T_d can be defined as follows:

$$T_{proposed} = \frac{1}{M}(t_{l_1} + t_{l_2} + \ldots + t_{l_M}), \tag{12}$$

where t_{l_i} is the decoding delay of l_i, neglecting the cost of CRC.

The worst-case scenario for t_{l_i} can be expressed as:

$$t_{l_i} = c \times L \times i \times \frac{N}{M} \log\left(i \times \frac{N}{M}\right). \tag{13}$$

Substituting Formula (13) into Formula (12), the worst-case average decoding delay for the proposed decoder in this paper can be obtained.

The ratio of average decoding delays (R_{delay}) between the two decoding methods can be expressed as:

$$R_{delay} = \frac{T_{proposed}}{T_{CA-SCL}}. \tag{14}$$

Table 1 provides detailed values of the storage unit ratio (R_{mem}) and average decoding delay ratio (R_{delay}) for segmentation parameters M = 2 and 4, decoding paths L = 4, and polar codeword length N = 1024. These values are commonly used in communication systems. Compared to the CA-SCL decoder, the decoding method proposed in this paper shows a substantial reduction in both required storage units and decoding latency.

Table 1. The specific values of R_{mem} and $R_{\boldsymbol{delay}}$ under different parameters.

Parameters	M **= 2**	L **= 4**	N **= 1024**	M **= 4**	L **= 4**	N **= 1024**
$(R_{mem})_{worst}$		0.750			0.500	
R_{delay}		0.725			0.592	

3.4.3. Spectral Efficiency Analysis

Since the proposed method maps the CRCs to the OFDM pilots, no additional CRC is needed on the source vector. Consequently, compared with CA-SCL, the spectrum efficiency of the method presented here is also improved. Given the extremely limited spectrum resources in underwater acoustic communication, it is of utmost importance to enhance spectral efficiency.

Assuming the codeword length is N and the CRC length is L_{CRC}, the encoding rate can be increased by L_{CRC}/N. The improvement in spectral efficiency depends on the modulation scheme, which can be denoted as:

$$\lambda = \frac{L_{CRC}}{N_{FFT} \times \log_2(Q)}, \tag{15}$$

where Q is the information bits contained in each symbol. For example, using BPSK modulation, Q = 1; N_{FFT} is the FFT length; λ is the value of spectral efficiency improvement.

4. Numerical Simulations and Sea Trials

4.1. Numerical Simulation Results and Analysis

The parameters of the underwater OFDM acoustic communication system are detailed in Table 2. To address the mismatch between the codeword and the data rate, a puncturing method is implemented [24]. The length of the CPMDSSS aligns with the number of pilots used. Additionally, the decoding paths are configured with L = 16 for this system setup. The Gaussian construction method [15] was employed to establish reliable and unreliable bit channels of polar code.

The notation (M, S_{CRC}) denotes the division of the information bits into M segments, with each segment having a CRC of length S_{CRC}. Figure 4 shows the simulation results, comparing the proposed methods (4, 2) and (2, 4) with CA-SCL (1, 8) [8] in the additive

white Gaussian noise (AWGN) channel model. The results clearly demonstrate that the proposed decoder exhibits a slightly superior performance compared to CA-SCL. This improvement is attributed to the method's ability to identify decoding errors during the decoding process at an earlier stage, thereby increasing the likelihood of selecting the correct path and achieving a slightly superior performance. In addition, the use of polar code significantly improves the BER performance compared to uncoded MPSK [25].

Table 2. The parameters of the underwater OFDM acoustic communication system.

Parameter	Value	Parameter	Value
codeword length N	1024	data subcarriers	340
code rate	0.5	symbol duration	171 ms
sampling rate	48 kHz	FFT length	8192
bandwidth	4–8 kHz	cyclic prefix	43 ms
pilot subcarriers	340	modulation	QPSK

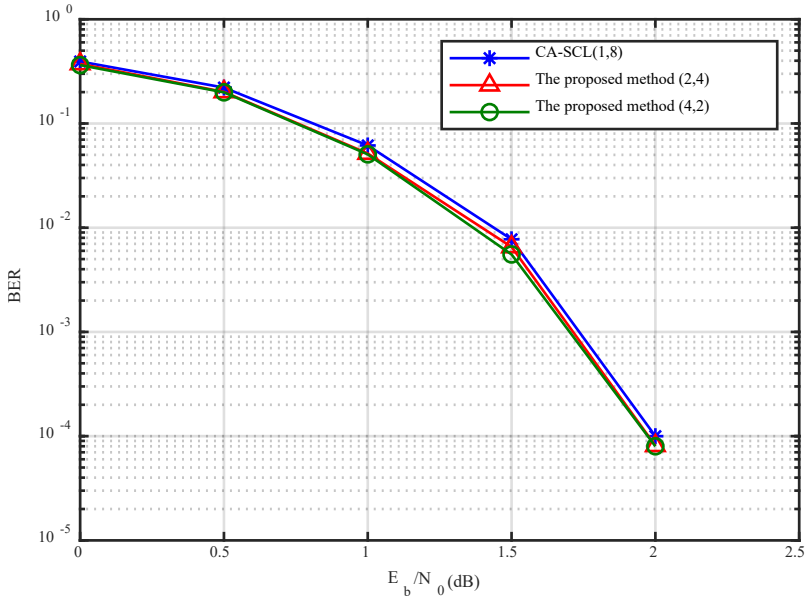

Figure 4. The simulation results of different decoding methods.

Table 3 presents the number of decoding paths required by the polar decoder during the simulation process. Compared to the proposed method, CA-SCL demands the maximum decoding paths, set at 16. As E_b/N_0 increases, the number of decoding paths required in the proposed method gradually decreases. This reduction is primarily due to the segmented approach used here, where information bits are divided into M segments. Each segment employs an adaptive decoding path. With higher E_b/N_0 values, the probability of successfully passing CRC during each decoding attempt increases, leading to a reduction in necessary decoding paths.

Table 3. The number of decoding paths required by the polar decoder.

E_b/N_0	0	0.5	1	1.5	2
CA-SCL (1, 8)	16	16	16	16	16
Proposed method (2, 4)	14.46	14.71	9.23	5.15	1.99
Proposed method (4, 2)	14.59	14.04	7.38	3.22	1.43

Compared to the proposed method (2, 4), the proposed method (4, 2) achieves further reduction in decoding paths. The main reason is that, as M increases, the number of information bits in each segment decreases, allowing for timely CRC and increasing the probability

of correct decoding, thereby reducing the required decoding paths. Consequently, the method (4, 2) exhibits the fewest decoding paths among the evaluated configurations.

In comparison to CA-SCL, the proposed method (4, 2) achieves an impressive 80% reduction in decoding paths, indicating a significant decrease in storage requirements and decoding complexity.

4.2. Sea Trial Results and Analysis

To validate the feasibility and reliability of the proposed method, sea trials of underwater acoustic communication were conducted. The experiment involved transmitting signals over a distance of approximately 11 km, with the underwater transducer submerged to a depth of about 100 m. The parameters of the communication system corresponded to those detailed in Table 2. Additionally, Figure 5 depicts the sound velocity profile of the experimental area.

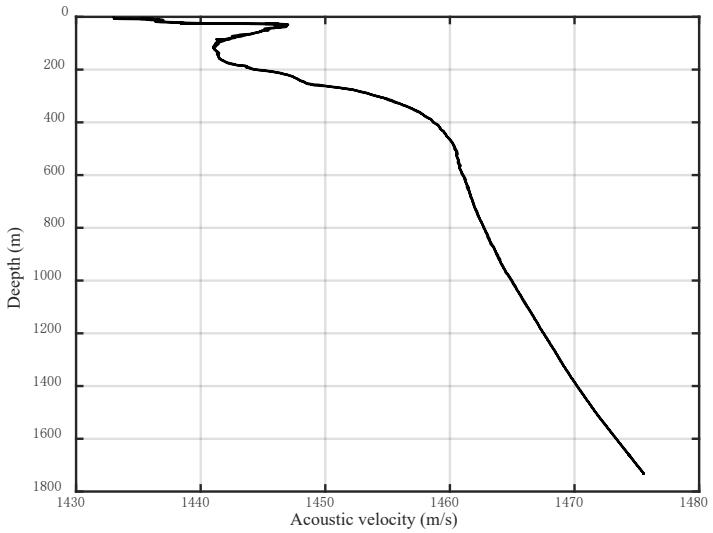

Figure 5. The sound velocity profile of the experimental area.

We conducted correlation analysis between the local copies and the received CPMDSSS obtained in step 1 of Section 3.3. The local copy with the highest correlation was chosen as the demodulated spread spectrum sequence, allowing us to obtain the CRC for each information segment. Figure 6 illustrates the correlation coefficient, depicting the correlation among different local copies and the received CPMDSSS. In this figure, an amplitude corresponding to 0 on the horizontal axis represents self-correlation, while non-zero amplitudes on the horizontal axis indicate cross-correlation. It can be seen that the selected sequence exhibits high self-correlation and low cross-correlation, which facilitates accurate CRC demodulation.

Table 4 presents the average decoding bit error rate (BER), the average number of decoding paths, and the average decoding delay for various decoding methods. The SC decoder, offering only one selectable decoding path, exhibits the lowest average decoding delay but the highest average BER. In contrast, both the proposed method and CA-SCL, configured with decoding paths set to $L = 16$, have more average decoding paths than the SC decoder, resulting in higher average decoding delays. However, their average decoding BERs are lower than the SC decoder, with both less than 10^{-3}.

Compared to the CA-SCL decoding method, the proposed method reduces the average decoding paths by approximately 71%, and the average decoding delay is reduced by 64%. This reduction is primarily attributed to the utilization of segmented CRC and the incorporation of an adaptive path decoding method, which effectively decreases the average decoding delay, aligning with the theoretical analysis.

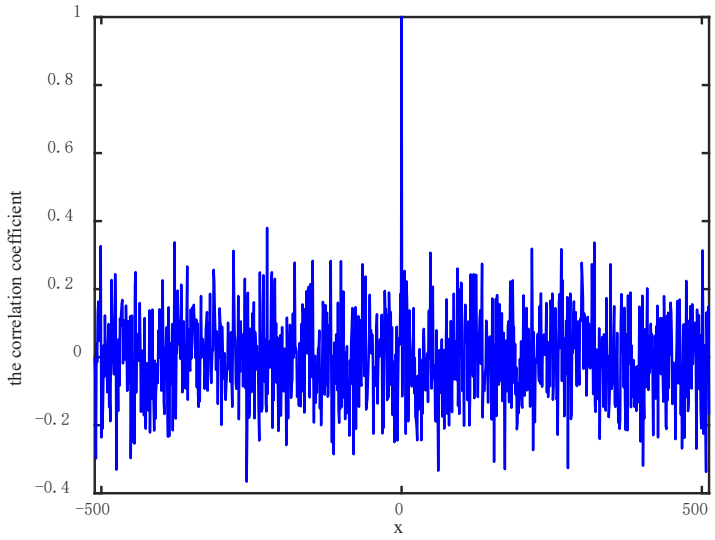

Figure 6. The correlation coefficient of the CPM sequences.

Table 4. The average decoding BERs for different decoding methods.

Decoding Method	Average Decoding BER	Average Decoding Paths	Average Decoding Delay (s)
SC	3.14×10^{-3}	1	0.0116
CA-SCL	7.56×10^{-4}	16	0.0667
The proposed method (4, 2)	7.23×10^{-4}	4.52	0.0234

5. Conclusions

To address the issues of CA-SCL requiring a large number of storage units, a long decoding delay, and low spectral efficiency, this paper proposes a CPMDSSS-assisted adaptive serial cancellation list decoding method for underwater OFDM acoustic communication. The theoretical analysis and simulation results demonstrate the efficacy of the proposed method in reducing the required storage units and decoding delays while enhancing spectral efficiency. Moreover, the empirical sea trial results confirm that the proposed method achieves significant reductions in average decoding delays while maintaining a low bit error rate. This method represents a high-performance, low-complexity decoding solution for polar codes.

Author Contributions: Conceptualization, Y.S. and D.H.; methodology, Y.S. and J.L.; experiments, D.L. and D.H.; data analysis, Y.S. and D.H.; writing—original draft preparation, Y.S.; writing—review and editing, D.H. and J.L.; funding acquisition, Y.S. All authors have read and agreed to the published version of the manuscript.

Funding: This research was funded by Natural Science Foundation of Fujian Province, (Grant No. 2023J05247), MinJiang University Science Project (Grant No. MJY23012), Fujian Provincial Department of Education Young and Middle-aged Teacher Education Research Project (Science and Technology) (Grant No. JAT222031).

Institutional Review Board Statement: Not applicable.

Informed Consent Statement: Not applicable.

Data Availability Statement: Data are contained within the article.

Conflicts of Interest: The authors declare no conflicts of interest.

References

1. Arikan, E. Channel Combining and Splitting for Cutoff Rate Improvement. *IEEE Trans. Inf. Theory* **2006**, *52*, 628–639. [CrossRef]
2. Chiu, M.-C. Analysis and Design of Polar-Coded Modulation. *IEEE Trans. Commun.* **2022**, *70*, 1508–1521. [CrossRef]

3. Han, S.; Kim, B.; Ha, J. Rate-Compatible Punctured Polar Codes. *IEEE Commun. Lett.* **2022**, *26*, 753–757. [CrossRef]
4. Shen, Y.; Zhou, W.; Huang, Y.; Zhang, Z.; You, X.; Zhang, C. Fast Iterative Soft-Output List Decoding of Polar Codes. *IEEE Trans. Signal Process.* **2022**, *70*, 1361–1376. [CrossRef]
5. Chen, C.; Zhang, X.; Liu, Y.; Wang, W.; Zeng, Q. An Ultra-Low Comsplexity Early Stopping Criterion for Belief Propagation Polar Code Decoder. *IEEE Commun. Lett.* **2022**, *26*, 723–727. [CrossRef]
6. Arikan, E. Channel Polarization: A Method for Constructing Capacity-Achieving Codes for Symmetric Binary-Input Memoryless Channels. *IEEE Trans. Inf. Theory* **2009**, *55*, 3051–3073. [CrossRef]
7. Tal, I.; Vardy, A. List Decoding of Polar Codes. *IEEE Trans. Inf. Theory* **2015**, *61*, 2213–2226. [CrossRef]
8. Niu, K.; Chen, K. CRC-Aided Decoding of Polar Codes. *IEEE Commun. Lett.* **2012**, *16*, 1668–1671. [CrossRef]
9. Zhou, H.; Zhang, C.; Song, W.; Xu, S.; You, X. Segmented CRC-Aided SC List Polar Decoding. In Proceedings of the 2016 IEEE 83rd Vehicular Technology Conference (VTC Spring), Nanjing, China, 15–18 May 2016; pp. 1–5.
10. Ercan, F.; Condo, C.; Hashemi, S.A.; Gross, W.J. On Error-Correction Performance and Implementation of Polar Code List Decoders for 5G. In Proceedings of the 2017 55th Annual Allerton Conference on Communication, Control, and Computing (Allerton), Monticello, IL, USA, 3–6 October 2017; pp. 443–449.
11. Hashemi, S.A.; Condo, C.; Gross, W.J. Simplified Successive-Cancellation List Decoding of Polar Codes. In Proceedings of the 2016 IEEE International Symposium on Information Theory (ISIT), Barcelona, Spain, 10–15 July 2016; pp. 815–819.
12. Hashemi, S.A.; Condo, C.; Gross, W.J. Fast Simplified Successive-Cancellation List Decoding of Polar Codes. In Proceedings of the 2017 IEEE Wireless Communications and Networking Conference Workshops (WCNCW), San Francisco, CA, USA, 19–22 March 2017; pp. 1–6.
13. Li, B.; Shen, H.; Tse, D. An Adaptive Successive Cancellation List Decoder for Polar Codes with Cyclic Redundancy Check. *IEEE Commun. Lett.* **2012**, *16*, 2044–2047. [CrossRef]
14. Trifonov, P. Efficient Design and Decoding of Polar Codes. *IEEE Trans. Commun.* **2012**, *60*, 3221–3227. [CrossRef]
15. Kraidy, G.M. Performance Analysis of Low Density Parity-Check Codes over the Bernoulli-Gaussian Channel. In Proceedings of the 2019 16th Canadian Workshop on Information Theory (CWIT), Hamilton, ON, Canada, 2–5 June 2019; pp. 1–5.
16. Balatsoukas-Stimming, A.; Parizi, M.B.; Burg, A. LLR-Based Successive Cancellation List Decoding of Polar Codes. *IEEE Trans. Signal Process.* **2015**, *63*, 5165–5179. [CrossRef]
17. Wang, P.; Yang, Q.; Hu, Y.; Xiong, J.; Jia, Y.; Guo, D. A Novel Voting Model Based on Parity Check Equations for Blind Detection of M-Sequences. *IEEE Access* **2024**, *12*, 34131–34140. [CrossRef]
18. Liu, S.; Zhou, Z.; Adhikary, A.R.; Yang, Y. New Supersets of Zadoff-Chu Sequences via the Weil Bound. *Cryptogr. Commun.* **2023**, *16*, 89–108. [CrossRef]
19. Wu, L.; Yin, X.; Chen, H.; Chen, P.; Fang, Y. Differential Pulse-Position Modulation for Multi-User Chaotic Communication. *IEEE Trans. Veh. Technol.* **2024**, 1–15. [CrossRef]
20. Li, C.; Marzani, F.; Yang, F. Demodulation of Chaos Phase Modulation Spread Spectrum Signals Using Machine Learning Methods and Its Evaluation for Underwater Acoustic Communication. *Sensors* **2018**, *18*, 4217. [CrossRef] [PubMed]
21. Umar, T.; Nadeem, M.; Anwer, F. Modified Chaotic Quadratic Map with Improved Robust Region. *Int. J. Inf. Tecnol.* **2024**, *16*, 131–136. [CrossRef]
22. Rugini, L. Linear Equalization for Multicode MC-CDMA Downlink Channels. *IEEE Commun. Lett.* **2012**, *16*, 1353–1356. [CrossRef]
23. Hara, S.; Prasad, R. Overview of Multicarrier CDMA. *IEEE Commun. Mag.* **1997**, *35*, 126–133. [CrossRef]
24. Wang, R.; Liu, R. A Novel Puncturing Scheme for Polar Codes. *IEEE Commun. Lett.* **2014**, *18*, 2081–2084. [CrossRef]
25. Rugini, L. SEP Bounds for MPSK With Low SNR. *IEEE Commun. Lett.* **2020**, *24*, 2473–2477. [CrossRef]

Disclaimer/Publisher's Note: The statements, opinions and data contained in all publications are solely those of the individual author(s) and contributor(s) and not of MDPI and/or the editor(s). MDPI and/or the editor(s) disclaim responsibility for any injury to people or property resulting from any ideas, methods, instructions or products referred to in the content.